

# Elastic $\alpha$ - $^{12}\text{C}$ scattering at low energies with the resonant $2_2^+$ and $2_3^+$ states of $^{16}\text{O}$

Shung-Ichi Ando<sup>1</sup>,

*Department of Display and Semiconductor Engineering,  
Research Center for Nano-Bio Science,  
Sunmoon University, Asan, Chungnam 31460, Republic of Korea*

The elastic  $\alpha$ - $^{12}\text{C}$  scattering for  $l = 2$  at low energies is studied in an effective Lagrangian approach. We explicitly include two resonant  $2_2^+$  and  $2_3^+$  states of  $^{16}\text{O}$  in the scattering amplitudes and construct an  $S$  matrix assuming that three amplitudes, non-resonant part of the amplitude which has the sub-threshold  $2_1^+$  state of  $^{16}\text{O}$  and those of the two resonant states, are represented by the summation of corresponding parts of the phase shift. Then, we fit the parameters in the  $S$  matrix to the phase shift data by imposing three conditions at the very low energies where the phase shift data are not available. By using the fitted parameters, we calculate the asymptotic normalization coefficients (ANC) of the  $2_1^+$  state of  $^{16}\text{O}$  and find that the previously reported small and large values of the ANC can be reproduced depending on the imposed conditions, but we obtain large error bars for the large ANC values which are reported from the  $\alpha$  transfer reactions.

PACS(s): 11.10.Ef, 24.10.-i, 25.55.-e, 26.20.Fj

---

<sup>1</sup><mailto:sando@sunmoon.ac.kr>

## 1. Introduction

Radiative  $\alpha$  capture on carbon-12,  $^{12}\text{C}(\alpha,\gamma)^{16}\text{O}$ , is an essential reaction in nuclear astrophysics, which determines the  $^{12}\text{C}/^{16}\text{O}$  ratio in stars [1]. Over the last half-century, many experimental and theoretical studies for the reaction have been carried out. See, e.g., Refs. [2, 3, 4, 5, 6, 7] for review.

Direct measurement of the reaction at the Gamow-peak energy,  $E_G = 0.3$  MeV, in stars, where  $E$  is the kinetic energy of  $\alpha$ - $^{12}\text{C}$  system in the center of mass frame, is not easy because the Gamow penetration factor becomes vanishingly small; one needs to extrapolate the reaction rate to  $E_G$  by employing a theoretical formula and the experimental data measured at a few MeV or larger. The radiative capture reaction at  $E_G$  is known to be  $E1$  and  $E2$  transitions dominant because of the sub-threshold  $1_1^-$  and  $2_1^+$  ( $J_{i-th}^\pi$ ) states of  $^{16}\text{O}$ , whose binding energies are  $E(1_1^-) = -0.045$  MeV and  $E(2_1^+) = -0.245$  MeV, respectively, from the  $\alpha$ - $^{12}\text{C}$  breakup threshold energy. In our previous works, we have studied elastic  $\alpha$ - $^{12}\text{C}$  scattering with and without sub-threshold states of  $^{16}\text{O}$  for  $l = 0, 1, 2, 3$  [8, 9] and the inclusion of ground  $0_1^+$  state and resonant  $0_3^+$  state of  $^{16}\text{O}$  for  $l = 0$  [10, 11] along with the  $E1$  transition of  $^{12}\text{C}(\alpha,\gamma)^{16}\text{O}$  and  $\beta$  delayed  $\alpha$  emission from  $^{16}\text{N}$  [7, 12] in effective field theory (EFT). In this work, we study the inclusion of resonant  $2_2^+$  and  $2_3^+$  states of  $^{16}\text{O}$  in the calculation of elastic  $\alpha$ - $^{12}\text{C}$  scattering for  $l = 2$ .<sup>2</sup>

A problem of the calculation of elastic  $\alpha$ - $^{12}\text{C}$  scattering for  $l = 2$  at low energies in EFT [8, 9, 14], and also in the other calculations in which the effective range expansion is adopted [15], is small values of asymptotic normalization coefficient (ANC) of the  $2_1^+$  state of  $^{16}\text{O}$ . A typical value of the ANC using the effective range expansion is  $|C_b| \simeq 2 \times 10^4$  fm $^{-1/2}$ . It is significantly smaller than those obtained from the  $\alpha$ -transfer reactions,  $|C_b| = (1.14 \sim 1.82) \times 10^5$  fm $^{-1/2}$  [16, 17, 18, 19], and those from other theoretical calculations; e.g., Sparenberg obtained  $|C_b| = 1.445 \times 10^5$  fm $^{-1/2}$  from phase-equivalent super-symmetric potentials [20], and Dufour and Descouvemont did  $|C_b| = 1.26 \times 10^5$  fm $^{-1/2}$  from generator coordinate method [21]. The difference in the ANC values will be consequential in an estimate of the  $E2$  transition of  $^{12}\text{C}(\alpha,\gamma)^{16}\text{O}$  at  $E_G$ . The ANC values of the  $2_1^+$  state of  $^{16}\text{O}$  for other approaches are well summarized in Table XIII in Ref. [5] and Table VI in Ref. [21].

In this work, we investigate the elastic  $\alpha$ - $^{12}\text{C}$  scattering for  $l = 2$  at low energies including the resonant  $2_2^+$  and  $2_3^+$  states of  $^{16}\text{O}$  in the study so that we can use the whole phase shift data for  $l = 2$  at  $2.6 \leq E_\alpha \leq 6.62$  MeV reported in Ref. [22] for the parameter fit, where  $E_\alpha$  is the  $\alpha$  energy in the lab frame. We separate the phase shift into three parts: those for the non-resonant part including the sub-threshold  $2_1^+$  state and for the two resonant parts of the  $2_2^+$  and  $2_3^+$  states of  $^{16}\text{O}$ . We also study the inclusion of a contribution from the resonant  $2_4^+$  state of  $^{16}\text{O}$  as a background contribution from high energy, to fit a tail of the phase shift data at the high energy side. An aim of the present work is how we can reproduce the large ANC values reported in the  $\alpha$  transfer reactions by using the phase shift data. For this aim, we introduce three conditions (I), (II), (III) (we will mention them in detail in section 4) to be applied to the inverse of the non-resonant part

---

<sup>2</sup>A preliminary result of this work was reported in Ref. [13].

of  $^{16}\text{O}$  propagator,  $D_2(p)$ , at  $0 \leq E_\alpha \leq 2.6$  MeV, where the experimental data are not available. Then, we fit the parameters to the data and calculate the ANC of the  $2_1^+$  state of  $^{16}\text{O}$ . We find that the parameters are fitted very well to the experimental phase shift data for all the conditions (I), (II), (III), where the  $\chi^2/N$  values for the parameter fit are less than one or almost one for all cases; the both small and large ANC values, depending on the choice of the conditions, are reproduced by using the fitted parameters. Thus, it is not clear how one can pin down the value of ANC of the  $2_1^+$  state of  $^{16}\text{O}$  from the phase shift data of elastic  $\alpha$ - $^{12}\text{C}$  scattering. As already discussed in the literature, additional experimental input may be necessary to determine the value of ANC of the  $2_1^+$  state of  $^{16}\text{O}$ .

The present work is organized as follows. In section 2, an expression for the  $S$  matrix is introduced and an effective Lagrangian is presented, and the elastic scattering amplitudes for  $l = 2$  are derived from the Lagrangian in section 3. In section 4, we discuss that three conditions are imposed in low energy regions where the experimental data do not exist and numerical results are obtained, and results and discussion of this work are presented in section 5.

## 2. $S$ matrix and effective Lagrangian

The  $S$  matrix of elastic  $\alpha$ - $^{12}\text{C}$  scattering for  $d$ -wave channel is given as

$$S_2 = e^{2i\delta_2}, \quad (1)$$

where  $\delta_2$  is the phase shift for the  $d$ -wave elastic scattering whose experimental values at  $2.6 \leq E_\alpha \leq 6.62$  MeV are reported in Ref. [22]. The scattering amplitude  $\tilde{A}_2$  is related to the  $S$  matrix as <sup>3</sup>

$$S_2 = 1 + 2ip\tilde{A}_2. \quad (2)$$

Because two resonant  $2_2^+$  and  $2_3^+$  states of  $^{16}\text{O}$  appear in the data at  $E_\alpha(2_2^+) = 3.58$  MeV and  $E_\alpha(2_3^+) = 5.81$  MeV, respectively, we may decompose the phase shift  $\delta_2$  as [23]

$$\delta_2 = \delta_2^{(nr)} + \delta_2^{(rs1)} + \delta_2^{(rs2)}, \quad (3)$$

where  $\delta_2^{(nr)}$  is the phase shift for the background-like, non-resonant part and  $\delta_2^{(rs1)}$  and  $\delta_2^{(rs2)}$  are those for the resonant  $2_2^+$  and  $2_3^+$  states of  $^{16}\text{O}$ , respectively. We assume that each of those phase shifts may have a relation to a corresponding scattering amplitude as

$$e^{2i\delta_2^{(ch)}} = 1 + 2ip\tilde{A}_2^{(ch)}, \quad (4)$$

where  $ch(annel) = nr, rs1, rs2$ , and  $\tilde{A}_2^{(nr)}$ ,  $\tilde{A}_2^{(rs1)}$ , and  $\tilde{A}_2^{(rs2)}$ , are the amplitudes for the non-resonant part, the first resonant part, and the second resonant part of the amplitudes, which will be constructed from the effective Lagrangian in below. Thus, the total

---

<sup>3</sup>There is a common factor difference between the expression of the amplitude  $\tilde{A}_2$  and the standard form of the amplitude  $A_2$ ;  $A_2 = \frac{10\pi}{\mu} e^{2i\sigma_2} \tilde{A}_2$  where  $\sigma_2$  is the Coulomb phase shift for  $l = 2$ ,  $e^{2i\sigma_2} = \Gamma(3 + i\eta)/\Gamma(3 - i\eta)$  with  $\eta = \kappa/p$ .

amplitude  $\tilde{A}_2$  for the nuclear reaction part in terms of the three amplitudes,  $\tilde{A}_2^{(nr)}$ ,  $\tilde{A}_2^{(rs1)}$ ,  $\tilde{A}_2^{(rs2)}$ , is

$$\tilde{A}_2 = \tilde{A}_2^{(nr)} + e^{2i\delta_2^{(nr)}} \tilde{A}_2^{(rs1)} + e^{2i(\delta_2^{(nr)} + \delta_2^{(rs1)})} \tilde{A}_2^{(rs2)}. \quad (5)$$

An effective Lagrangian to derive the scattering amplitude for the  $d$ -wave elastic  $\alpha$ - $^{12}\text{C}$  scattering at low energies including the sub-threshold  $2_1^+$  state of  $^{16}\text{O}$  and the resonant  $2_2^+$  and  $2_3^+$  states of  $^{16}\text{O}$  may be written as [8, 9, 10, 24]

$$\begin{aligned} \mathcal{L} = & \phi_\alpha^\dagger \left( iD_0 + \frac{\vec{D}^2}{2m_\alpha} \right) \phi_\alpha + \phi_C^\dagger \left( iD_0 + \frac{\vec{D}^2}{2m_C} \right) \phi_C \\ & + \sum_{k=0}^3 C_k^{(nr)} d_{(nr)ij}^\dagger \left[ iD_0 + \frac{\vec{D}^2}{2(m_\alpha + m_C)} \right]^k d_{(nr)ij} \\ & - y_{(nr)} \left[ d_{(nr)ij}^\dagger (\phi_\alpha O_{2,ij} \phi_C) + (\phi_\alpha O_{2,ij} \phi_C)^\dagger d_{(nr)ij} \right] \\ & + \sum_{N=1}^2 \sum_{k=0}^3 C_k^{(rsN)} d_{(rsN)ij}^\dagger \left[ iD_0 + \frac{\vec{D}^2}{2(m_\alpha + m_C)} \right]^k d_{(rsN)ij} \\ & - \sum_{N=1}^2 y_{(rsN)} \left[ d_{(rsN)ij}^\dagger (\phi_\alpha O_{2,ij} \phi_C) + (\phi_\alpha O_{2,ij} \phi_C)^\dagger d_{(rsN)ij} \right], \quad (6) \end{aligned}$$

where  $\phi_\alpha$  ( $m_\alpha$ ) and  $\phi_C$  ( $m_C$ ) are scalar fields (masses) of  $\alpha$  and  $^{12}\text{C}$ , respectively.  $D^\mu$  is a covariant derivative,  $D^\mu = \partial^\mu + i\mathcal{Q}A^\mu$  where  $\mathcal{Q}$  is the charge operator and  $A^\mu$  is the photon field.  $d_{(nr)ij}$  and  $d_{(rsN)ij}$  with  $N = 1, 2$  are the composite fields of  $^{16}\text{O}$  consisting of  $\alpha$  and  $^{12}\text{C}$  fields for  $l = 2$  for the non-resonant part ( $nr$ ) representing the sub-threshold  $2_1^+$  state of  $^{16}\text{O}$ , and the two resonant parts ( $rs1$ ) and ( $rs2$ ) representing the first and second resonant  $2_2^+$  and  $2_3^+$  states of  $^{16}\text{O}$ , respectively, which are introduced for perturbative expansion around the unitary limit [25, 26, 27, 28]. The coupling constants of the non-resonant part of the amplitude,  $C_k^{(nr)}$  with  $k = 0, 1, 2, 3$ , correspond to the effective range parameters of elastic  $\alpha$ - $^{12}\text{C}$  scattering while the first coupling constant  $C_0^{(nr)}$  is fixed by using the binding energy of the sub-threshold  $2_1^+$  state of  $^{16}\text{O}$  and the other parameters are fitted to the experimental phase shift data with other parameters appearing in the  $S$  matrix. The coupling constants of the resonant parts,  $C_k^{(rs1)}$ , and  $C_k^{(rs2)}$  with  $k = 0, 1, 2, 3$ , are rewritten in terms of the first two terms,  $C_0^{(rs1)}$  and  $C_1^{(rs1)}$  as well as  $C_0^{(rs2)}$  and  $C_1^{(rs2)}$ , by using the resonant energies and widths for the resonant  $2_2^+$  and  $2_3^+$  states of  $^{16}\text{O}$ , respectively. The third and fourth parameters for the resonant  $2_3^+$  state,  $C_2^{(rs2)}$  and  $C_3^{(rs2)}$  are fitted to the phase shift data while we set  $C_2^{(rs1)} = C_3^{(rs1)} = 0$  for the first resonant  $2_2^+$  state of  $^{16}\text{O}$ . The coupling constants  $y_{(nr)}$  and  $y_{(rsN)}$  with  $N = 1, 2$  are uniquely defined but convention-dependent [29]. We take the convenient choice;  $y_{(nr)} = y_{(rs1)} = y_{(rs2)} = \sqrt{2\pi/\mu}$  where  $\mu$  is the reduced mass of  $\alpha$  and  $^{12}\text{C}$ , as a trade-off for a complicated redefinition of the respective composite fields.

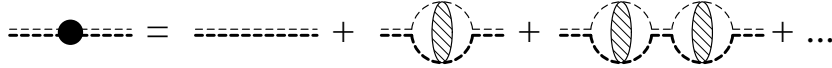


Figure 1: Diagrams for dressed  $^{16}\text{O}$  propagator. A thick (thin) dashed line represents a propagator of  $^{12}\text{C}$  ( $\alpha$ ), and a thick and thin double dashed line with and without a filled circle represent a dressed and bare  $^{16}\text{O}$  propagator, respectively. A shaded blob represents a set of diagrams consisting of all possible one-potential-photon-exchange diagrams up to infinite order and no potential-photon-exchange one.

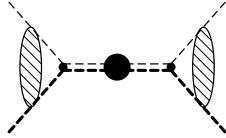


Figure 2: Diagram of the scattering amplitude. See the caption of Fig. 1 as well.

The scattering amplitudes,  $\tilde{A}_2^{(nr)}$  and  $\tilde{A}_2^{(rsN)}$  with  $N = 1, 2$ , are calculated from the diagrams depicted in Figs. 1 and 2. Here, the bubble diagrams are summed up to the infinite order in Fig. 1. For the non-resonant part of the amplitude, we treat it non-perturbatively because of the study for the ANC of  $2_1^+$  state of  $^{16}\text{O}$  at its binding energy. For the resonant parts of the amplitude (for our case, they are classified as narrow resonances because of  $\Gamma_r \ll E_r$  [30]), the counting rules of resonant states are carefully studied by Gelman [23] and Habashi et al. [30]. The energy range of phase shift data covers the two resonant states, and at the vicinities of the resonant energies we should have the amplitudes for which the bubble diagrams are summed up to the infinite order. While at the off-resonant energy regions, one can expand the resonant amplitudes perturbatively and the  $d_{(nr)ij}$  and  $d_{(rsN)ij}$  with  $N = 1, 2$  fields may start mixing through the bubble diagram for corrections at higher orders. We keep the summed amplitudes for the resonant states as leading contributions and ignore the field mixing in the present study.

### 3. Scattering amplitudes

For the non-resonant amplitude  $\tilde{A}_2^{(nr)}$ , we have [8, 9]

$$\tilde{A}_2^{(nr)} = \frac{C_\eta^2 W_2(p)}{K_2(p) - 2\kappa H_2(p)}, \quad (7)$$

where the function  $C_\eta^2 W_2(p)$  in the numerator of the amplitude is calculated from the initial and final state Coulomb interactions in Fig. 2;  $p$  is the magnitude of relative momentum of the  $\alpha$ - $^{12}\text{C}$  system in the center of mass frame,  $p = \sqrt{2\mu E}$ . Thus, one has

$$C_\eta^2 = \frac{2\pi\eta}{\exp(2\pi\eta) - 1}, \quad (8)$$

$$W_2(p) = \frac{1}{4}(\kappa^2 + p^2)(\kappa^2 + 4p^2), \quad (9)$$

where  $\eta = \kappa/p$ :  $\kappa$  is the inverse of the Bohr radius,  $\kappa = Z_2 Z_6 \alpha_E \mu$ , where  $Z_n$  are the number of protons of the nuclei,  $Z_2 = 2$  and  $Z_6 = 6$ , and  $\alpha_E$  is the fine structure constant. The function  $-2\kappa H_2(p)$  in the denominator of the amplitude is the Coulomb self-energy term which is calculated from the loop diagram in Fig. 1, and one has

$$H_2(p) = W_2(p)H(\eta), \quad H(\eta) = \psi(i\eta) + \frac{1}{2i\eta} - \log(i\eta), \quad (10)$$

where  $\psi(z)$  is the digamma function. The nuclear interaction is represented in terms of the effective range parameters in the function  $K_2(p)$  in the denominator of the amplitude in Eq. (7). As discussed in Ref. [8], large and significant contributions to the series of effective range expansion, compared to that evaluated from the phase shift data at the lowest energy of the data,  $E_\alpha = 2.6$  MeV, appear from the Coulomb self-energy term,  $-2\kappa H_2(p)$ . To subtract those contributions, we include the effective range terms up to  $p^6$  order as counterterms. For more detail, see the appendix. Thus, we have

$$K_2(p) = -\frac{1}{a_2} + \frac{1}{2}r_2 p^2 - \frac{1}{4}P_2 p^4 + Q_2 p^6, \quad (11)$$

where  $a_2, r_2, P_2, Q_2$  are effective range parameters.

Now we fix a parameter among the four effective range parameters,  $a_2, r_2, P_2$ , and  $Q_2$ , by using the condition that the inverse of the scattering amplitude  $\tilde{A}_2^{(nr)}$  vanishes at the binding energy of the sub-threshold  $2_1^+$  state of  $^{16}\text{O}$ . Thus, the denominator of the scattering amplitude,

$$D_2(p) = K_2(p) - 2\kappa H_2(p), \quad (12)$$

vanishes at  $p = i\gamma$  where  $\gamma$  is the binding momentum of the  $2_1^+$  state of  $^{16}\text{O}$ ;  $\gamma = \sqrt{2\mu B_2}$  where  $B_2$  is the binding energy of the  $2_1^+$  state of  $^{16}\text{O}$  from the  $\alpha$ - $^{12}\text{C}$  breakup threshold. Using the condition,  $D_2(i\gamma) = 0$ , we fix the effective range parameter  $a_2$  as

$$-\frac{1}{a_2} = \frac{1}{2}\gamma^2 r_2 + \frac{1}{4}\gamma^4 P_2 + \gamma^6 Q_2 + 2\kappa H_2(i\gamma). \quad (13)$$

Using the relation in Eq. (13), we rewrite the denominator of the amplitude  $D_2(p)$  as

$$D_2(p) = \frac{1}{2}r_2(\gamma^2 + p^2) + \frac{1}{4}P_2(\gamma^4 - p^4) + Q_2(\gamma^6 + p^6) + 2\kappa [H_2(i\gamma) - H_2(p)], \quad (14)$$

where we have three constants,  $r_2, P_2, Q_2$ , in the function  $D_2(p)$  for the non-resonant amplitude  $\tilde{A}_2^{(nr)}$ , which are fitted to the phase shift data.

For the elastic scattering amplitudes for the resonant  $2_2^+$  and  $2_3^+$  states of  $^{16}\text{O}$ , we may first have those amplitudes as the same expression of the non-resonant amplitude in Eq. (7) in terms of the effective range expansion as

$$\tilde{A}_2^{(rsN)} = \frac{C_\eta^2 W_2(p)}{K_2^{(rsN)}(p) - 2\kappa H_2(p)}, \quad (15)$$

with  $N = 1, 2$ , which correspond to the first and second resonant  $2_2^+$  and  $2_3^+$  states of  $^{16}\text{O}$ , respectively, and

$$K_2^{(rsN)}(p) = -\frac{1}{a_2^{(rsN)}} + \frac{1}{2}r_2^{(rsN)}p^2 - \frac{1}{4}P_2^{(rsN)}p^4 + Q_2^{(rsN)}p^6. \quad (16)$$

We now introduce the expansion around the resonant energies in the denominator of the scattering amplitudes [31]. Thus, we rewrite the amplitudes as

$$\tilde{A}_2^{(rsN)} = -\frac{1}{pE - E_r^{(rsN)} + R^{(rsN)}(E) + i\frac{1}{2}\Gamma^{(rsN)}(E)}, \quad (17)$$

with

$$\Gamma^{(rsN)}(E) = \Gamma_r^{(rsN)} \frac{pW_2(p)C_\eta^2}{p_rW_2(p_r)C_{\eta_r}^2}, \quad (18)$$

$$R^{(rs2)}(E) = a(E - E_r^{(rs2)})^2 + b(E - E_r^{(rs2)})^3, \quad (19)$$

and  $R^{(rs1)}(E) = 0$ , where

$$a = \frac{1}{2}Z_r \left( 2P_2^{(rs2)}\mu^2 - 48Q_2^{(rs2)}\mu^3 E_r^{(rs2)} + 2\kappa Re \left. \frac{\partial^2 H_2}{\partial E^2} \right|_{E=E_r^{(rs2)}} \right), \quad (20)$$

$$b = \frac{1}{6}Z_r \left( -48Q_2^{(rs2)}\mu^3 + 2\kappa Re \left. \frac{\partial^3 H_2}{\partial E^3} \right|_{E=E_r^{(rs2)}} \right), \quad (21)$$

$$Z_r^{-1} = Re \left. \frac{\partial}{\partial E} D_2^{(rs2)}(E) \right|_{E=E_r^{(rs2)}}, \quad Z_r = \frac{\Gamma_r^{(rs2)}}{2p_rW_2(p_r)C_{\eta_r}^2}. \quad (22)$$

In the above equations,  $E_r^{(rsN)}$  and  $\Gamma_r^{(rsN)}$  with  $N = 1, 2$  are the energies and the widths of the resonant states of  $^{16}\text{O}$ , and  $p_r$  are the resonant momenta,  $p_r = \sqrt{2\mu E_r^{(rsN)}}$ , which also appear in  $\eta_r$  as  $\eta_r = \kappa/p_r$ .

Using the expression of the amplitudes in Eqs. (7) and (17), we have the  $S$  matrix as

$$e^{2i\delta_2} = \frac{K_2(p) - 2\kappa Re H_2(p) + ipC_\eta^2 W_2(p)}{K_2(p) - 2\kappa Re H_2(p) - ipC_\eta^2 W_2(p)} \times \frac{E - E_r^{(rs1)} - i\frac{1}{2}\Gamma^{(rs1)}(E)}{E - E_r^{(rs1)} + i\frac{1}{2}\Gamma^{(rs1)}(E)} \frac{E - E_r^{(rs2)} + R^{(rs2)}(E) - i\frac{1}{2}\Gamma^{(rs2)}(E)}{E - E_r^{(rs2)} + R^{(rs2)}(E) + i\frac{1}{2}\Gamma^{(rs2)}(E)}. \quad (23)$$

We will fit the parameters in the  $S$  matrix to the phase shift data by using the sine function of the phase shift,  $f = \sin(\delta_2)$ , in the next section; the scattering cross section is proportional to  $\sin^2(\delta_2)$ . For the study of the ANC, at the small energy region, the exponential factors in Eq. (5) almost become one due to the Gamow factor in  $C_\eta^2$ , and the amplitude becomes

$$\tilde{A}_2 = \tilde{A}_2^{(nr)} + \tilde{A}_2^{(rs1)} + \tilde{A}_2^{(rs2)} + O(C_\eta^4), \quad (24)$$

where the pole at the  $2_1^+$  state of  $^{16}\text{O}$  exists in  $\tilde{A}_2^{(nr)}$ , the ANC  $|C_b|$  for the  $2_1^+$  state of  $^{16}\text{O}$  is calculated by using a formula [32]

$$|C_b| = \frac{1}{2}\gamma^2\Gamma(3 + \kappa/\gamma) \left[ -\frac{\partial D_2(p)}{\partial p^2} \Big|_{p^2=-\gamma^2} \right]^{-1/2}, \quad (25)$$

where  $\Gamma(z)$  is the gamma function.

#### 4. Numerical results

Nine parameters,  $\theta = \{r_2, P_2, Q_2, E_r^{(rs1)}, \Gamma_r^{(rs1)}, E_r^{(rs2)}, \Gamma_r^{(rs2)}, a, b\}$ , appear in the  $S$  matrix, where  $r_2$ ,  $P_2$ , and  $Q_2$  are the effective range parameters, which reproduce the binding energy of the sub-threshold  $2_1^+$  state of  $^{16}\text{O}$  in  $\tilde{A}_2^{(nr)}$ ,  $E_r^{(rs1)}$  and  $\Gamma_r^{(rs1)}$  are the resonant energy and width of the  $2_2^+$  state of  $^{16}\text{O}$  in  $\tilde{A}_2^{(rs1)}$ , and  $E_r^{(rs2)}$  and  $\Gamma_r^{(rs2)}$  are those of the  $2_3^+$  state of  $^{16}\text{O}$  in  $\tilde{A}_2^{(rs2)}$ . While  $a$  and  $b$  are the coefficients of higher order terms  $(E - E_r^{(rs2)})^n$  with  $n = 2, 3$  in the  $R^{(rs2)}(E)$  function, respectively, obtained expanding the denominator of  $\tilde{A}_2^{(rs2)}$  around the resonant energy,  $E = E_r^{(rs2)}$ . We treat the parameters  $a$  and  $b$  as independent parameters for the sake of simplicity though they are functions of  $P_2^{(rs2)}$ ,  $Q_2^{(rs2)}$  and  $E_r^{(rs2)}$ . As mentioned in the introduction, we also study the inclusion of  $2_4^+$  state of  $^{16}\text{O}$ ; this can be done straightforwardly. The expression for the  $2_4^+$  state of  $^{16}\text{O}$  in the  $S$  matrix is the same as that for the  $2_2^+$  state of  $^{16}\text{O}$  in Eq. (23), but we use the fixed experimental values of the energy and width,  $E_r^{(rs3)}$  and  $\Gamma_r^{(rs3)}$ . Thus, we employ two expressions of the  $S$  matrix for the parameter fit; one is the  $S$  matrix given in Eq. (23), and the other is that including the contribution from the  $2_4^+$  state of  $^{16}\text{O}$ . We fit the nine parameters in the  $S$  matrices (by using the fitting function  $f = \sin(\delta_2)$ , as mentioned above) to the phase shift data  $\delta_2$  of the elastic  $\alpha$ - $^{12}\text{C}$  scattering for  $d$ -wave channel reported by Tischhauser et al. [22], by employing an Markov chain Monte Carlo (MCMC) program [33].

In addition, to investigate the difference between the large ANC values obtained from the  $\alpha$  transfer reactions and the small ANC values from the effective range expansion, we impose three different conditions to the inverse of the  $^{16}\text{O}$  propagator,  $D_2(p)$ , of the non-resonant amplitude at the very low  $\alpha$  energy region,  $0 < E_\alpha < 2.6$  MeV, where the experimental data are not available. We note that the function  $D_2(p)$  should be negative at  $0 < E_\alpha < 2.6$  MeV. Those three conditions are

- (I)  $D_2(p) < 0$ ,
- (II)  $D_2(p_{i+1}) < D_2(p_i)$ ,
- (III)  $\frac{dD_2}{dp^2} \Big|_{p=p_{i+1}} < \frac{dD_2(p)}{dp^2} \Big|_{p=p_i}$ ,

where  $p_{i+1} > p_i$  and  $p = \sqrt{2\mu E} = \sqrt{1.5\mu E_\alpha}$ . The first condition (I) is always required because there should be no zeros for no resonant states of  $^{16}\text{O}$  at the very low energy region. The second condition (II) is modest and the condition (III) can reproduce the large ANC values reported from the  $\alpha$  transfer reactions as we will see below. We note



	(I)	(II)	(III)
$r_2$ (fm <sup>-3</sup> )	0.137(4)	0.150(4)	0.159(4)
$P_2$ (fm <sup>-1</sup> )	-1.36(5)	-1.18(4)	-1.07(4)
$Q_2$ (fm)	0.013(16)	0.075(12)	0.112(11)
$E_r^{(rs1)}$ (MeV)	2.68308(5)	2.68309(5)	2.68309(5)
$\Gamma_r^{(rs1)}$ (keV)	0.75(2)	0.74(2)	0.74(2)
$E_r^{(rs2)}$ (MeV)	4.3549(1)	4.3545(1)	4.3544(1)
$\Gamma_r^{(rs2)}$ (keV)	74.66(3)	74.60(3)	74.57(3)
$a$ (MeV <sup>-1</sup> )	0.20(6)	0.47(6)	0.59(5)
$b$ (MeV <sup>-2</sup> )	0.94(5)	1.13(8)	1.39(10)
$ C_b $ (fm <sup>-1/2</sup> )	$2.0(2) \times 10^4$	$3.2(6) \times 10^4$	$11(26) \times 10^4$
$\chi^2/N$	0.74	0.86	1.13

Table 1: Values and errors of nine parameters  $\{r_2, P_2, Q_2, E_r^{(rs1)}, \Gamma_r^{(rs1)}, E_r^{(rs2)}, \Gamma_r^{(rs2)}, a, b\}$  in the  $S$  matrix in Eq. (23) fitted to the experimental phase shift  $\delta_2$  of elastic  $\alpha$ -<sup>12</sup>C scattering for  $l = 2$  using the conditions (I), (II), (III) at the low energy region. The ANC,  $|C_b|$ , for the  $2_1^+$  states of <sup>16</sup>O are calculated by using the fitted values of the parameters, and values of  $\chi^2/N$ , where  $N$  is the number of data, for the fit are presented in the last row of the table.

that those conditions are easily included as conditions in the prior distribution with the MCMC method.

For the parameter fit, we treat the set of the parameters,  $\theta = \{r_2, P_2, Q_2, E_r^{(rs1)}, \Gamma_r^{(rs1)}, E_r^{(rs2)}, \Gamma_r^{(rs2)}, a, b\}$  as free parameters while the values of  $r_2, P_2, Q_2$  are constrained due to the conditions (I), (II), (III) in the inverse of the <sup>16</sup>O propagator,  $D_2(p)$ . For the initial values of the parameters,  $r_2, P_2, Q_2$ , we employ the values reported by Sparenberg, Capel, and Baye [34];  $r_2 = 0.1580$  fm<sup>-3</sup>,  $P_2 = -1.041$  fm<sup>-1</sup>,  $Q_2 = 0.1411$  fm, which lead to a large ANC value,  $|C_b| = 13.8 \times 10^4$  fm<sup>-1/2</sup>. We also choose the initial values of  $a$  and  $b$  as  $a = 0.1(0.5)$  MeV<sup>-1</sup> and  $b = 1.1(0.5)$  MeV<sup>-2</sup> for the  $S$  matrix without (with) the  $2_4^+$  state of <sup>16</sup>O. While we use the center values of the experimental resonant energies and widths of the  $2_2^+$  and  $2_3^+$  states of <sup>16</sup>O;  $E_r^{(rs1)} = 2.6826(5)$  MeV,  $\Gamma_r^{(rs1)} = 0.625(100)$  keV,  $E_r^{(rs2)} = 4.358(4)$  MeV,  $\Gamma_r^{(rs2)} = 71(3)$  keV [35], as initial values for the parameter fit. We use the fixed experimental values for the energy and width of the  $2_4^+$  state of <sup>16</sup>O as  $E_r^{(rs3)} = 5.858$  MeV and  $\Gamma_r^{(rs3)} = 150$  keV [35]. Details for the parameter fit and the calculation of the error bars can be found in our previous work [36].

We are now in a position to discuss the numerical results of the present work. In Tables 1 and 2, we present the values and errors of the parameters in the  $S$  matrices without and with the contribution from the  $2_4^+$  state of <sup>16</sup>O, respectively, fitted to the phase shift data imposing the three conditions (I), (II), (III). We also include in the tables the values and errors of the ANC,  $|C_b|$ , of the  $2_1^+$  state of <sup>16</sup>O and the  $\chi^2/N$  values where  $N$  is the number of data,  $N = 354$ .

	(I)	(II)	(III)
$r_2$ (fm <sup>-3</sup> )	0.149(4)	0.152(4)	0.159(3)
$P_2$ (fm <sup>-1</sup> )	-1.19(5)	-1.16(4)	-1.07(3)
$Q_2$ (fm)	0.081(16)	0.090(14)	0.121(9)
$E_r^{(rs1)}$ (MeV)	2.68308(5)	2.68308(5)	2.68309(5)
$\Gamma_r^{(rs1)}$ (keV)	0.75(2)	0.75(2)	0.75(2)
$E_r^{(rs2)}$ (MeV)	4.3545(2)	4.3545(1)	4.3542(1)
$\Gamma_r^{(rs2)}$ (keV)	74.61(3)	74.59(3)	74.55(3)
$a$ (MeV <sup>-1</sup> )	0.46(12)	0.51(10)	0.71(6)
$b$ (MeV <sup>-2</sup> )	0.47(9)	0.53(10)	0.81(11)
$ C_b $ (fm <sup>-1/2</sup> )	$3.1(6) \times 10^4$	$3.6(9) \times 10^4$	$13(30) \times 10^4$
$\chi^2/N$	0.66	0.69	0.73

Table 2: Values and errors of nine parameters  $\{r_2, P_2, Q_2, E_r^{(rs1)}, \Gamma_r^{(rs1)}, E_r^{(rs2)}, \Gamma_r^{(rs2)}, a, b\}$  in the  $S$  matrix, which contains the contribution from the  $2_4^+$  state of  $^{16}\text{O}$ , fitted to the experimental phase shift  $\delta_2$  of elastic  $\alpha$ - $^{12}\text{C}$  scattering for  $l = 2$  using the conditions (I), (II), (III) at the low energy region. See the caption of Table 1 as well.

In the tables, one can see that the values of  $\chi^2/N$  increase as the conditions (I), (II), (III) are orderly changed. This is caused by tighter restrictions being applied to the effective range parameters,  $r_2, P_2, Q_2$ , as altering the conditions (I), (II), (III) in order. Nevertheless, all values of the parameters may be regarded to be fitted very well to the phase shift data because the values of  $\chi^2/N$  are smaller than one or almost one whereas the inclusion of the  $2_4^+$  state of  $^{16}\text{O}$  makes the  $\chi^2/N$  values in Table 2 smaller than those in Table 1.

The fitted parameters in the tables can be parted into two groups depending on sensitivities to the conditions (I), (II), (III). One can easily see that the energies and widths of the resonant states of  $^{16}\text{O}$  are insensitive to the conditions; they are determined by the significant resonant peaks. We find that the fitted values of  $E_r^{(rs1)}, \Gamma_r^{(rs1)}, E_r^{(rs2)}, \Gamma_r^{(rs2)}$ , basically agree with the experimental values [35]. The fitted values of  $r_2, P_2, Q_2, a, b$  are sensitive to the conditions (I), (II), (III); they are fitted to the non-resonant part of the phase shift data at the energy regions below the first resonant state and between the two resonant states. One may notice that the values of  $b$  in Table 2 are remarkably smaller than those in Table 1, apparently due to the effect of the  $2_4^+$  state of  $^{16}\text{O}$ . We can reproduce the small and large values of the ANC,  $|C_b|$ , of the  $2_1^+$  state of  $^{16}\text{O}$  by using the fitted values of the effective range parameters,  $r_2, P_2, Q_2$  for the conditions (I), (II), (III), where the effective range parameters for the condition (III) reasonably agree well with those reported by Sparenberg, Capel, and Baye for the large ANC value. In addition, a very large error bar appears in the large ANC value, so the small and large values of the ANC in fact agree with each other within the error bars. In the present study, therefore, it is not easy to pin down which of the ANC values is correct because of the error bars of

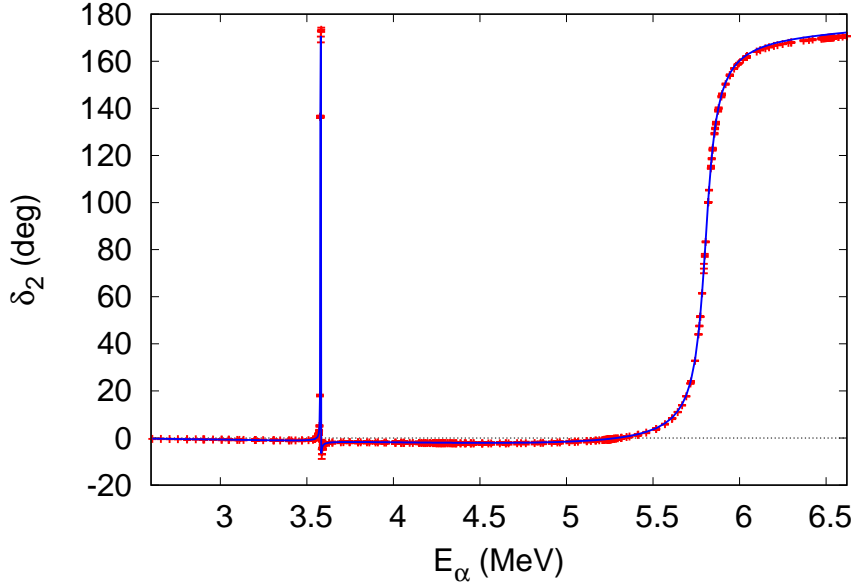


Figure 3: Phase shift  $\delta_2$  of elastic  $\alpha$ - $^{12}\text{C}$  scattering for  $d$ -wave channel as a function of  $E_\alpha$  calculated by using the fitted values of the parameters in the (I) column in Table 1. Experimental data are included in the figure as well.

the ANC values and the  $\chi^2/N$  values discussed above.

In Fig. 3, we plot the phase shift  $\delta_2$  of elastic  $\alpha$ - $^{12}\text{C}$  scattering for  $d$ -wave channel calculated by using the fitted values of the parameters in the (I) column in Table 1 as a function of the  $\alpha$  energy,  $E_\alpha$ , and the phase shift data are also included in the figure. This is a typical figure for almost all of the cases; two peaks of the resonant  $2_2^+$  and  $2_3^+$  states of  $^{16}\text{O}$  are well reproduced. The differences due to the values of the fitted parameters are hardly seen at the low energy tail and the energies between the two resonant states.

In Figs. 4 and 5, we plot the curves of the phase shift  $\delta_2$  for the small  $\delta_2$  values,  $-5^\circ \leq \delta_2 \leq 5^\circ$ , which are calculated by using the values of the parameters in the  $S$  matrices without and with the  $2_4^+$  state of  $^{16}\text{O}$ , respectively, fitted to the phase shift data for the low energy tail and the energies between the two resonant states. The phase shift data are included in the figures as well. One can see that the calculated curves agree very well within the error bars of the data as discussed above that the  $\chi^2/N$  values are less than one or almost one for all the cases.

In Fig. 6, we plot the real part of  $D_2(p)$  calculated by using the values of the parameters in Table 1 (as curves) and in Table 2 (as dashed curves) for the conditions (I), (II), (III) as a function of  $E_\alpha$  at  $0 \leq E_\alpha \leq 2.6$  MeV, where the phase shift data are not available. One can see that those curves satisfy the conditions (I), (II), (III) and go through the quite different values of  $\text{Re}D_2(p)$  at an energy range,  $0 \leq E_\alpha \leq 1.5$  MeV whereas the inclusion

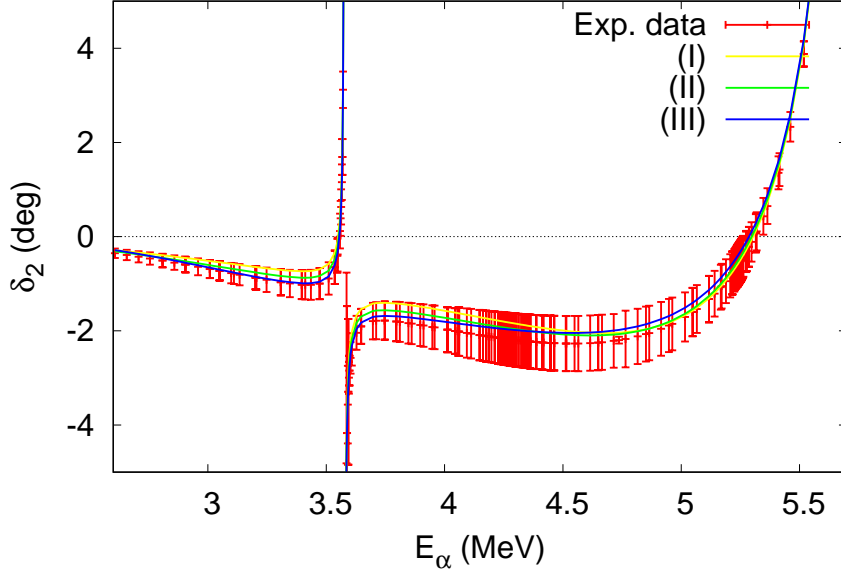


Figure 4: Phase shift  $\delta_2$  of elastic  $\alpha$ - $^{12}\text{C}$  scattering for  $d$ -wave channel at the small phase shift region as a function of  $E_\alpha$  calculated by using the fitted values of the parameters in Table 1. Experimental data are included in the figure as well.

of the  $2_4^+$  state of  $^{16}\text{O}$  makes the curve of (I) less deviated from the other curves. When one calculates the  $E2$  transition rate of  $^{12}\text{C}(\alpha, \gamma)^{16}\text{O}$  at  $E_G$ , i.e.,  $E_\alpha = \frac{4}{3}E_G = 0.4$  MeV, the center value of  $ReD_2(p)$  for the condition (III) becomes extremely tiny, much smaller than the errors of  $ReD_2(p)$ . This will lead to a large uncertainty in an estimate of the  $E2$  transition rate of  $^{12}\text{C}(\alpha, \gamma)^{16}\text{O}$  with the large ANC values.

## 5. Results and discussion

In this work, we studied the elastic  $\alpha$ - $^{12}\text{C}$  scattering for the  $d$ -wave channel at the low energy region including the first and second  $d$ -wave resonant states, the  $2_2^+$  and  $2_3^+$  states of  $^{16}\text{O}$ , in an effective Lagrangian approach. The phase shift  $\delta_2$  is separated into three; one is for the non-resonant part which contains the sub-threshold  $2_1^+$  state of  $^{16}\text{O}$ , and the other two parts are for the two resonant  $2_2^+$  and  $2_3^+$  states of  $^{16}\text{O}$ . We include four effective range parameters,  $a_2$ ,  $r_2$ ,  $P_2$ ,  $Q_2$ , in each of the three amplitudes (thus 12 parameters in total) due to the modification of the counting rules discussed in the appendix as well as in Ref. [8], while we employed the nine parameters  $\{r_2, P_2, Q_2, E_r^{(rs1)}, \Gamma_r^{(rs1)}, E_r^{(rs2)}, \Gamma_r^{(rs2)}, a, b\}$  as free parameters because  $a_2$  is fixed by using the binding energy of the  $2_1^+$  state of  $^{16}\text{O}$  and two of them ( $a$  and  $b$  for  $\tilde{A}_2^{(rs1)}$ ) turned out to be insensitive to the parameter fit. We also introduce a contribution from the  $2_4^+$  state of  $^{16}\text{O}$  as a background from high energy using the fixed experimental energy and width,  $E_r^{(rs3)}$  and  $\Gamma_r^{(rs3)}$ . To study the issue of the scattered, large and small values of the ANC, we introduce the three conditions (I),

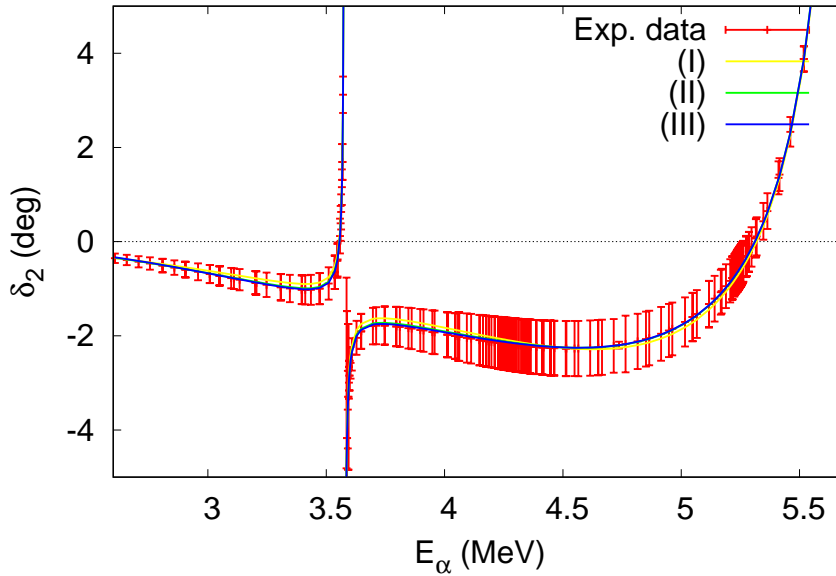


Figure 5: Phase shift  $\delta_2$  of elastic  $\alpha$ - $^{12}\text{C}$  scattering for  $d$ -wave channel at the small phase shift region as a function of  $E_\alpha$  calculated by using the fitted values of the parameters in Table 2. Experimental data are included in the figure as well.

(II), (III) at the very low energy region where the phase shift data are not available. The nine parameters in the  $S$  matrices with and without the  $2_4^+$  state of  $^{16}\text{O}$  are fitted to the phase shift data applying one of the three conditions.

For all the six cases of the parameter fit, the parameters are fitted very well to the data where the  $\chi^2/N$  values are less than one or almost one. The fitted values of the energies and widths of the two resonant states do not depend on the choice of the conditions, and our fitted values of the energies and widths basically agree with the experimental values. Those of the effective range parameters,  $r_2$ ,  $P_2$ ,  $Q_2$ , and the parameters  $a$  and  $b$  turned out to be sensitive to the choice of the conditions (and  $b$  is the most sensitive to the contribution from the  $2_4^+$  state of  $^{16}\text{O}$ ); they are fitted to the phase shift data at the non-resonance region, at the energies below the first resonant state and between the two resonant states. By using the fitted values of the effective range parameters, we can reproduce the both small and large values of the ANC,  $|C_b|$ , depending on the choice of the conditions. We also find the large error bars for the large ANC values. Therefore, it is not easy to clearly pin down the value of ANC from the phase shift data due to the large error bars of the ANC values and the  $\chi^2/N$  values for the parameter fit mentioned above.

The problem with fitting the parameters to the phase shift data for  $d$ -wave channel is that though the two resonant peaks are well reproduced as seen in Fig. 3, it is essential to

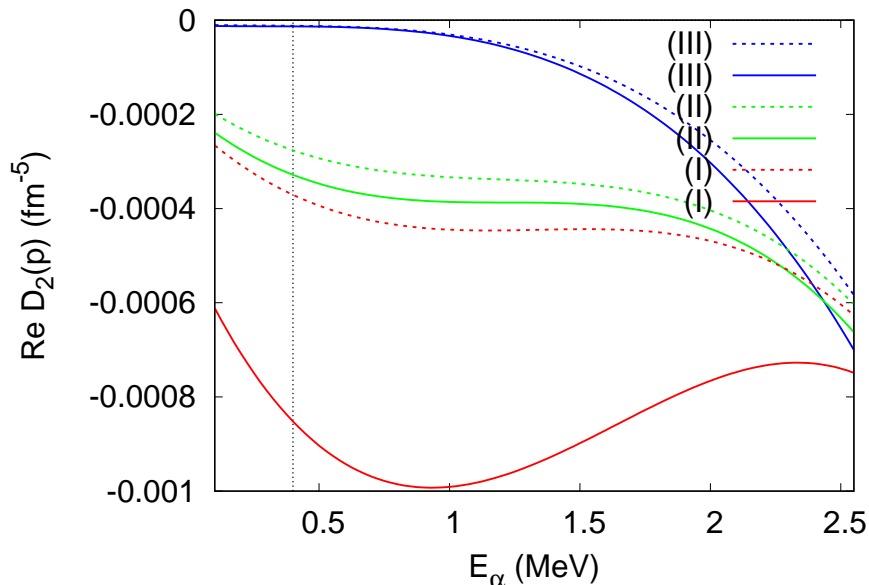


Figure 6: Real part of inverse of dressed  $^{16}\text{O}$  propagator for  $l = 2$ ,  $D_2(p)$ , calculated by using the values of the parameters with the conditions (I), (II), (III) in Table 1 (curves) and in Table 2 (dashed curves) as a function of  $E_\alpha$  at the energies where the experimental data are not available. A dotted vertical line at  $E_\alpha = 0.4$  MeV is also drawn in the figure.

fit the parameters to the tiny data at the low energy tail and the energy region between the two resonant states for the study of the ANC of the  $2_1^+$  state of  $^{16}\text{O}$ . Because the size of those data is so small compared to the distance between the binding energy of the sub-threshold  $2_1^+$  state of  $^{16}\text{O}$  and the lowest energy of the phase shift data,  $E_\alpha = 2.6$  MeV, it is not easy to clarify how much the fitting procedures work well when a number of parameters of a polynomial function are fitted to the data. This may be seen as an ambiguity of the curves of  $\text{Re}D_2(p)$  plotted in Fig. 6.

Apart from the ambiguity mentioned above, we reproduced the center values for the small and large ANC values using the conditions (I) and (III), respectively, in the tables 1 and 2. Because the error bar of the large ANC turns out to be very large, it is not so sure that we could reproduce the large ANC value from the phase shift data of  $\alpha$ - $^{12}\text{C}$  scattering for  $d$ -wave channel. Thus, as discussed in the literature, the value of ANC of the sub-threshold  $2_1^+$  state of  $^{16}\text{O}$  may need to be fixed by using other experimental data, such as the  $\alpha$  transfer reactions, e.g.,  $^{12}\text{C}(^6\text{Li},d)^{16}\text{O}^*(2_1^+)$  and  $^{12}\text{C}(^7\text{Li},t)^{16}\text{O}^*(2_1^+)$ , a cascade transition,  $^{12}\text{C}(\alpha,\gamma)^{16}\text{O}^*(2_1^+)$ , and a radiative decay of the excited state,  $^{16}\text{O}^*(2_1^+) \rightarrow ^{16}\text{O}_{g.s.} + \gamma$ , for the present approach. Those data may determine the value of ANC and provide a consistency check for a theoretical framework to estimate the  $E2$  transition of  $^{12}\text{C}(\alpha,\gamma)^{16}\text{O}$  at  $E_G$ .

## Acknowledgements

This work was supported by the Basic Research Program through the National Research Foundation of Korea funded by the Ministry of Education of Korea (NRF-2019R1F1A1040362).

## Appendix

In this appendix, we discuss a renormalization procedure for the effective range terms due to large and significant contributions from the Coulomb self-energy term,  $-2\kappa H_2(p)$ , for the  $d$ -wave scattering. It has been discussed for the  $s$ -wave scattering in Ref. [8].

At the energy region below the resonant energies, where one may assume that the resonant parts of the amplitudes are negligible, one can make a relation between the phase shift  $\delta_2$  and the non-resonant part of the amplitude as

$$C_\eta^2 W_2(p) p \cot \delta_2 = K_2(p) - 2\kappa \text{Re} H_2(p), \quad (26)$$

where the function  $K_2(p)$  is represented as an effective range expansion, and the Coulomb self-energy term,  $-2\kappa H_2(p)$ , can be expanded in powers of  $p^2/\kappa^2$  too. Thus, one has

$$-2\kappa \text{Re} H_2(p) = \frac{1}{24} \kappa^3 p^2 + \frac{51}{240} \kappa p^4 + \frac{191}{1008} \frac{p^6}{\kappa} - \frac{289}{10080} \frac{p^8}{\kappa^3} + \dots \quad (27)$$

At the smallest energy of the experimental data,  $E_\alpha = 2.6$  MeV, where  $p = \sqrt{2\mu E} = \sqrt{1.5\mu E_\alpha} = 104$  MeV, one can check the series of the terms in Eq. (27) converge; those terms numerically become

$$-2\kappa \text{Re} H_2(p = 104 \text{ MeV}) = 0.022 + 0.021 + 0.003 - 0.0009 + \dots \quad (\text{fm}^{-5}). \quad (28)$$

While the phase shift  $\delta_2$  at  $E_\alpha = 2.6$  MeV is  $\delta_2 = -0.0116^\circ$  [22], and the left-hand-side of Eq. (26) becomes

$$C_\eta^2 W_2(p) p \cot \delta_2 \Big|_{p=104\text{MeV}} = -0.019 \text{ fm}^{-5}. \quad (29)$$

Because the first and second terms in the r.h.s of Eq. (28) obtained from the Coulomb self-energy term are in the same order of magnitude as that calculated from the experimental phase shift data in Eq. (29), one needs to subtract them by including the corresponding effective range terms at  $p^2$  and  $p^4$  orders in  $K_2(p)$  as counterterms. In addition, to control sub-leading corrections we include the effective range term at  $p^6$  order in  $K_2(p)$  as well.

## References

- [1] W. A. Fowler, Rev. Mod. Phys. **56**, 149 (1984).
- [2] L. R. Buchmann and C. A. Barnes, Nucl. Phys. A **777**, 254 (2006).
- [3] A. Coc, F. Hammache, J. Kiener, Eur. Phys. J. A **51**, 34 (2015).
- [4] C. A. Bertulani and T. Kajino, Prog. Part. Nucl. Phys. **89**, 56 (2016).

- [5] R. J. deBoer *et al.*, Rev. Mod. Phys. **89**, 035007 (2017), and references therein.
- [6] H.-W. Hammer, S. Konig, and U. van Kolck, Rev. Mod. Phys. **92**, 25004 (2020).
- [7] S.-I. Ando, Eur. Phys. J. A **57**, 17 (2021).
- [8] S.-I. Ando, Phys. Rev. C **97**, 014604 (2018).
- [9] S.-I. Ando, Eur. Phys. J. A **52**, 130 (2016).
- [10] S.-I. Ando, J. Korean Phys. Soci. **73**, 1452 (2018).
- [11] S.-I. Ando, Phys. Rev. C **102**, 034611 (2020).
- [12] S.-I. Ando, Phys. Rev. C **100**, 015807 (2019).
- [13] S.-I. Ando, Few-Body Syst. **62**, 55 (2021).
- [14] S. Konig, D. Lee, and H.-W. Hammer, J. Phys. G: Nucl. Part. Phys. **40**, 045106 (2013).
- [15] Yu. V. Orlov, B. F. Irgaziev, and L. I. Nikitina, Phys. Rev. C **93**, 014612 (2016).
- [16] C. R. Brune, W. H. Geist, R. W. Kavanagh, and K. D. Veal, Phys. Rev. Lett. **83**, 4025 (1999).
- [17] A. Belhout et al., Nucl. Phys. A **793**, 178 (2007).
- [18] S. Adhikari and C. Basu, Phys. Lett. B **682**, 216 (2009).
- [19] M. L. Avila et al., Phys. Rev. Lett. **114**, 071101 (2015).
- [20] J.-M. Sparenberg, Phys. Rev. C **69**, 034601 (2004).
- [21] M. Dufour and P. Descouvemont, Phys. Rev. C **78**, 015808 (2008).
- [22] P. Tischhauser *et al.*, Phys. Rev. C **79**, 055803 (2009).
- [23] B. Gelman, Phys. Rev. C **80**, 034005 (2009).
- [24] S.-I. Ando, Eur. Phys. J. A **33**, 185 (2007).
- [25] H. A. Bethe, Phys. Rev. **76**, 38 (1949).
- [26] D. B. Kaplan, Nucl. Phys. B **494**, 471 (1997).
- [27] S. R. Beane and M. J. Savage, Nucl. Phys. A **694**, 511 (2001).
- [28] S. Ando and C. H. Hyun, Phys. Rev. C **72**, 014008 (2005).
- [29] H. W. Griesshammer, Nucl. Phys. A **744**, 192 (2004).



- [30] J. B. Habashi, S. Fleming, and U. van Kolck, *Eur. Phys. J. A* **57**, 169 (2021).
- [31] R. Higa, H.-W. Hammer, and U. van Kolck, *Nucl. Phys. A* **809**, 171 (2008).
- [32] Z. R. Iwinski and L. Rosenberg, *Phys. Rev. C* **29**, 349 (1984).
- [33] D. Foreman-Mackey et al., *Pub. Astro. Soc. Pac.* **125**, 306 (2013).
- [34] J.-M. Sparenberg, P. Capel, and D. Baye, *Jour. Phys.: Conf. Seri.* **312**, 082040 (2011).
- [35] D. R. Tilley, H. R. Weller, and C. M. Cheves, *Nucl. Phys. A* **564**, 1 (1993).
- [36] H.-E. Yoon and S.-I. Ando, *J. Korean Phys. Soci.* **75**, 202 (2019).